EMBRY-RIDDLE
Aeronautical University™
SCHOLARLY COMMONS

Dissertations and Theses

5-2018

Propulsive Battery Packs Sizing for Aviation Applications

Tianyuan Zhao

Follow this and additional works at: https://commons.erau.edu/edt

Part of the Aerospace Engineering Commons

PROPULSIVE BATTERY PACKS SIZING FOR AVIATION APPLICATIONS

A Thesis

Submitted to the Faculty

of

Embry-Riddle Aeronautical University

by

Tianyuan Zhao

In Partial Fulfillment of the

Requirements for the Degree

of

Master of Science in Aerospace Engineering

May 2018

Embry-Riddle Aeronautical University

Daytona Beach, Florida

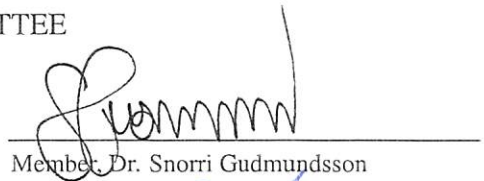PROPULSIVE BATTERY PACKS SIZING FOR AVIATION APPLICATIONS

by

Tianyuan Zhao

A Thesis prepared under the direction of the candidate's committee chairman, Dr. Richard P. Anderson, Department of Aerospace Engineering, and has been approved by the members of the thesis committee. It was submitted to the School of Graduate Studies and Research and was accepted in partial fulfillment of the requirements for the degree of Master of Science in Aerospace Engineering.
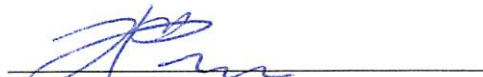
THESIS COMMITTEE
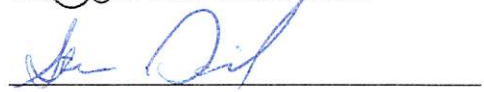
_____
Chairman, Dr. Richard P. Anderson

_____
Member, Dr. Jianhua Liu
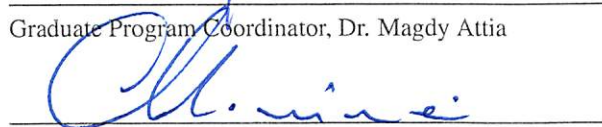
_____
Graduate Program Coordinator, Dr. Magdy Attia
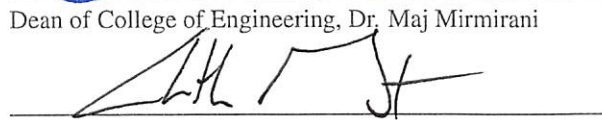
_____
Dean of College of Engineering, Dr. Maj Mirmirani

_____
Vice Chancellor, Academic Support, Dr. Christopher Grant

_____
Member, Dr. Snorri Gudmundsson

_____
Member, Dr. Steven Daniel

4.12.2018
_____
Date

4/16/18
_____
Date

4/18/18
_____
Date

ACKNOWLEDGMENTS

TABLE OF CONTENTS

LIST OF TABLES

LIST OF FIGURES

SYMBOLS

C	Battery C Rate
D	Drag
$E_{T/O}$	Takeoff Consumed Energy
E_{cr}	Cruise Consumed Energy
I	Current
L/D	Lift to Drag Ratio (Glide Ratio)
N_p	Number of Cells in Parallel
N_s	Number of Cells in Series
P	Power
q	Torque
Q_{batt}	Battery System Capacity
Q_{cell}	Battery Cell Capacity
R_I	Internal Resistance
T	Thrust
t	time
V	Voltage
v	Velocity (Airspeed)
η_{mot}	Electric Motor Efficiency
η_{prop}	Propeller Efficiency
W_o	Gross Weight

ABBREVIATIONS

AC	Alternative Current
CO_2	Carbon Dioxide
BMS	Battery Management System
CAFE	Competition in Aircraft Flight Efficiency
EFRC	Eagle Flight Research Center
EMF	Electro-Motive Force
Li-Ion	Lithium-Ion
NASA	The National Aeronautics and Space Administration
MEA	More Electric Aircraft
OCV	Open-Circuit Voltage
RPM	Revolution per Minute
SOC	State of Charge
TRL	Technology Readiness Level
UAV	Unmanned Aerial Vehicle

ABSTRACT

Zhao, Tianyuan MSAE, Embry-Riddle Aeronautical University, May 2018. PROPULSIVE

BATTERY PACKS SIZING FOR AVIATION APPLICATIONS.

This thesis derives analytical methods for sizing the propulsive battery packs for designing an electric-driven aircraft. Lithium-Ion (Li-Ion) battery is the primary choice of battery cell chemistry in this thesis research due to its superior specific energy and market availability. The characteristics of Lithium-Ion battery cells are first determined and studied using experimental test results and manufacturers published data. Based on the design requirement to the battery system, the battery sizing will fall into one of the two sizing categories. The first category is power sizing, which requires the battery's ability to deliver full power demanded by the electric motor. The second category is endurance sizing, which requires the battery system to store sufficient energy for the required endurance. Both types of sizing are analytically derived. From the sizing result, capacity is used to determine the parallel connected battery cells. The required system voltage governs the series connected cells. A battery discharging simulation model is built to validate the sizing results.

1. Introduction

1.1 Motivation

For over 100 years, aircraft have been using fossil fuels as the primary propulsion energy source. With the increasing environmental and noise concerns, clean and sustainable energy sources are gaining more attention around the world. The automotive industry is leading the evolution of technology by introducing many electric and hybrid vehicle models to the market.

A similar trend is expected in the aviation industry. In 2011, NASA, Google, and CAFE Foundation hosted the Green Flight Challenge. The Challenge intended to improve the energy efficiency, enhance safety, and reduce noise pollution for the future of aviation. Participating teams demonstrated various high-efficiency electric or hybrid propulsion systems (Tomazia, 2013). Embry-Riddle Aeronautical University's Eagle Flight Research Center (EFRC) also entered the challenge, whose hybrid-electric aircraft featured a direct-drive parallel-hybrid propulsion system.

All aircraft are sensitive to weight. The performance of an electric aircraft relies heavily on the performance of its battery system. Comparing the specific energy of battery cells with gasoline, one can easily realize that batteries are at a significant disadvantage in terms of specific energy. The advanced Li-Ion battery produced by Panasonic is able to provide 240 Wh/Kg specific energy (Panasonic, 2016), which seems insignificant amount when

facing gasoline's 12,000 Wh/Kg (Exxon, 2008). However, battery technology has been improving for many decades and specific energy continues to grow at a rate of 5 to 8 percent each year (Straubel, 2016). On the other hand, the peak energy efficiency of an alternate-current (AC) 3-phase electric motor can be as high as 93%, much more than the internal combustion engine's 35% (YASA, 2012) (Takaishi, Numata, Nakano, & Sakaguchi, 2008). This efficiency difference is further reducing the overall performance gap between electric and gas.

The sizing and designing of the battery system of an electric aircraft can have a significant impact on the design outcomes. The battery system's weight, volume, power output, and energy capacity can influence the electric aircraft's maneuverability, stability, range, and endurance. For fossil fuel driven aircraft, range and endurance equations, such as Breguet equations, yields closed-form solutions to size the fuel weight. However, aircraft design textbooks hardly mention the sizing of electrical propulsion system as any part of the design process.

For a fuel-driven aircraft, due to the weight reduction during flight, the relation between the range and sizing of the fuel system is non-linear. For an electric-driven aircraft, the weight of the battery system will remain unchanged throughout the entire mission profile. However, the power of a battery system is the product of the discharging current and the battery voltage. The voltage of the battery will decrease during discharge. Therefore, if assuming constant power is required for the cruise flight, the current draw from a battery system will increase throughout cruise flight. This behavior makes the battery pack sizing also a non-linear relationship with the cruise endurance requirement.

A fuel-driven aircraft can achieve higher power by increasing the air and fuel flow rate to the engine, but power output of a battery system is dependent on the voltage and the current output of the battery. To achieve higher power, one must increase the battery system's voltage or current. The voltage of a battery is constrained by the operating voltage range of the chosen battery chemistry type. The current output from any battery cell is also limited by the maximum C rating of the battery. Therefore, a power output rating will require a certain sizing of a battery system's capacity. This type of sizing is categorized as takeoff power sizing. These battery systems inherit a certain amount of endurance regardless of the design requirement of aircraft endurance.

In the cases when a design requires longer endurance than the takeoff sizing can provide, further increasing the battery system's capacity is needed. Therefore this sizing is categorized as cruise endurance sizing. This sizing method uses the total energy consumption to calculate the amount of capacity needed for the battery system. The number of battery cells in series can then be sized accordingly.

The Eagle Flight Research Center at Embry-Riddle Aeronautical University is at the forefront of the electric and hybrid aircraft research and development. Back in 2011, the Eco-Eagle Hybrid Stemme S-10 aircraft was engineered to compete in the Green Flight Challenge. It featured a patented direct drive parallel hybrid propulsion system. Nowadays, the EFRC is conducting the latest electric and hybrid aircraft research through the e-Spirit of St. Louis Project. This project converts a Diamond HK-36 powered glider into an all-electric driven aircraft. The battery system on this aircraft is fully designed and built by the students at the EFRC. This example will be used as a baseline to compare different battery

design approaches. At the same time, the EFRC is exploring the aircraft design space by implementing different types of hybrid propulsion system configurations to maximize system energy efficiency, reduce total CO_2 emission, extend flight range and endurance, and minimize noise footprint of aircraft. Much support was given by the industry for the research and development of hybrid and electric aircraft projects, which indicates public acceptance despite the low technology readiness level (TRL).

1.2 Problem Statement

Electric and hybrid electric aircraft have gained much interest globally due to the rising noise and pollution concerns generated by internal combustion engines. The sizing and design of propulsive battery systems are essential to the performance of electric or hybrid-electric aircraft. Extensive study is needed to evaluate how the battery pack sizing can impact an electric propulsion system. Therefore, this thesis focuses on the preliminary sizing of a propulsive battery system. First, the performance of battery cells will be reviewed and analyzed. Second, a sizing algorithm will be derived based on power or endurance requirement from the aircraft mission profile. A battery sizing tool will be developed based on the sizing algorithms. Third, the battery sizing will be categorized into novel zones defined here. An adequate battery sizing can either fall into a zone for takeoff power delivery or a zone for cruise endurance requirements. The closed-form equations defining the sizing zones will be derived for several aircraft applications. Finally, the potential of weight optimization will be evaluated through varying sizing parameters such as the nominal voltage and the cell type.

1.3 Objectives

1.3.1 General Objectives

This thesis focuses on creating an analytical method to size the propulsive battery system for a hybrid or a pure electric-driven aircraft. The emphasizes are the battery systems power output and the cruise endurance performances. The battery type to be studied and analyzed are 18650 Li-Ion cylindrical cells. However, the research methodology and algorithms can be extrapolated to any newest and greatest battery cell types. This analytical method first solves the number of cells necessary in the series connection to satisfy the system voltage requirement, then it solves the number of cells in parallel for the capacity requirement. The capacity requirement contains two types of sizing: takeoff power sizing and cruise endurance sizing. Battery sizings will fall into either type of sizing; it is determined by the specific sizing requirements.

1.3.2 Specific Objectives

Li-Ion Battery Characteristics Study and Analysis

The Li-Ion battery is one of the optimal selections of battery chemistry to be used as the aviation propulsive battery due to its higher specific energy compared to batteries with other chemistries. Li-Ion battery system with same weight can sustain a longer flight endurance than battery systems with other chemistry. However, Li-Ion batteries are sensitive to its discharging current. Manufacturers of Li-Ion batteries usually specify a current output

limit for any specific battery model to prevent overheating or thermal runaway issues. The output current is rated in terms of C, which is the capacity of the battery system.

During the discharge process of a Li-Ion battery, the voltage decreases with the decrease of remaining capacity. This is due to the chemical reaction's potential decreasing. In addition, Li-Ion battery's loading voltage further decreases when the battery is discharged at a higher current. This is due to the internal resistance dividing the voltage from the battery. The voltage behavior of the Li-Ion battery is critical to be considered since the voltage can drastically affect the performance of the electric aircraft. A voltage expression can be derived from battery testing data to express the voltage dynamics during a battery discharging process.

Propulsive Battery System Sizing Methodology

The number of battery cells connected in series in a battery system shall be sized by the acceptable system voltage of the electric drive-train components, namely the motor controller and the electric motor. When choosing the nominal voltage value, the designer shall take the voltage variation of the battery into consideration. This thesis will derive the sizing of series connected cells by the given acceptable voltage range of the electric system and the battery voltage throughout the discharge process.

The parallel number of battery cells in a battery system is determined by the capacity required from the system. Since the propulsive battery pack's current output is limited and the battery terminal voltage is passively determined by the remaining capacity and loading condition, only the capacity can be arbitrarily sized to satisfy the power requirement of the

system. The minimum feasible solution to an aircraft propulsive battery pack is to allow a single time of takeoff power at the beginning of the flight. The designer can also increase the number of parallel connected batteries to achieve a larger capacity such that the takeoff power is additionally available at a further stage of the flight. For this type of sizing, the battery pack's capacity inherits the ability to sustain a certain cruise endurance. Moreover, aircraft designers can size the battery pack when the mission profile requires an extended cruise endurance. For this type of sizing, the cruise endurance time required for the mission is longer than the inhered endurance from the takeoff power sizing. When sizing the battery system capacity, the value shall be the greater capacity from both takeoff power sizing and cruise endurance sizing.

With the battery systems voltage and the capacity determined, the total number of cells in parallel and series can be calculated. The battery system weight can be estimated using the cell weight and the empirical data of battery system weight fraction.

Battery System Sizing Strategy and Sizing Zones Definition

When both takeoff power and cruise endurance are required by the aircraft design criteria, the sizing of a propulsive battery system shall be evaluated under both requirements. The final propulsive battery sizing will be taken from the higher sizing result of the two. This way, the battery system will have both the required takeoff power and the cruise endurance performance.

As expected by the sizing methods, the sizing result will yield two different types. For the results which battery system is sized the takeoff power or cruise endurance the sizing

will fall into either the takeoff sizing zone or the cruise endurance sizing zone. Based on the zone definitions, closed-form equations for zone boundaries can be derived under reasonable assumptions. Furthermore, the crossing point between the two zones can be solved.

Weight Reduction Considerations

Additional weight reduction will be evaluated by varying the system parameters, such as the cells geometry or system voltage. Due to the discrete property when sizing the battery, weight fluctuation will occur when the system nominal voltage is slightly altered. The thesis will evaluate the weight fluctuation at a system level using the sizing result and the empirical weight fractions.

2. Technical and Literature Review

2.1 Lithium-Ion Battery Properties

Battery technology has come a long way. For batteries used in aviation, the battery's available power and specific energy are two of the main performance indexes. The specific energy of a battery has been increasing for many years as technology improves. The newest Lithium-Ion batteries have both high specific energy and specific power, which makes Lithium-Ion battery the ideal solution for the propulsive battery.

Lithium-Ion battery uses free-flowing Lithium ions stored in battery's anode and cathode as electron transporters to create electric potential. The different anode and cathode material selections give Lithium-Ion batteries different characteristics. Researchers have been working to find newer materials to replace existing ones in order to reduce overall cost and to improve performance and safety (Zhang & Zhang, 2015).

2.1.1 C Rating of Lithium-Ion Battery Cells

Battery cells with different chemistry usually have different C ratings. The C rate quantifies the charging or discharging current in terms of the battery's capacity. Regardless of the battery cell's size, discharging any battery cell at a 1C rate means the cell will deplete

from full charge in 1 hour. The formula below illustrates the relationship between capacity, current draw, and C rate. In this illustration, a 3.5 Ah battery is discharging at a rate of 2C:

$$I = Q \cdot C \qquad (2.1)$$

$$I = 3.5Ah \cdot 2/h \qquad (2.2)$$

$$I = 7A \qquad (2.3)$$

In equation 2.1, I is the discharging current, Q is the capacity of the particular cell used, and C is the C rate of the battery. The maximum current output is higher when the battery has a higher C rate. C rate will not change when battery cells are connected to a battery pack or system due to the fact that C rate disregard the capacity of the battery. Therefore the battery cell's C rate will also be the battery system's C rate. The amount of current is always the C multiple of the total capacity of the pack or system. Additionally, C rates provide an easier method to estimate the amount of time used for one full discharge of a particular battery type at the maximum current. The amount of time that will be used in one full charge or discharge is the reciprocal of the C rate. Such as illustrated in the equation 2.4, a 2C rated battery is used to calculate the estimation of time that will be used in a full discharge at the max C rate current.

$$t = \frac{1}{C} \qquad (2.4)$$

$$t = \frac{1}{2/h} \qquad (2.5)$$

$$t = 0.5h \qquad (2.6)$$

2.1.2   Series and Parallel Connections of Lithium-Ion Battery Cells

Lithium-Ion battery cells have many forms and shapes. Prismatic Lithium-Ion cells are commonly found in early portable electronics due to their light-weight characteristics. Larger pouch Lithium-Ion cells are commonly found in battery packs for powering electric vehicles (EV) and other high power devices due to lower manufacturing cost and ease of packaging. Both types of cells have safety concerns with prolonged use under heat and high current. Swelling and internal shortage are common causes of failure. When a Lithium-Ion battery fails, the chance of causing fire is high. Therefore, the consequences of Lithium-Ion battery failure can be catastrophic. The cylindrical Lithium-Ion cells, on the other hand, are normally contained by a stainless shell at the outer layer. This shell is able to prevent the external forces from damaging the internal components. Figure 2.1 shows a cylindrical Panasonic NCR-18650GA Lithium-Ion cell. The cell gets its name from its geometry of 18mm (0.71 in) diameter and 65mm height (2.56 in) (Panasonic, 2016)

Figure 2.1 Panasonic NCR-18650GA Lithium Ion Cell.

The Panasonic NCR-18650GA cell has 3.6V nominal voltage and 3500 mAh capacity. The propulsive battery pack for aviation application contains cells connected in series and parallel. The series connection is to provide sufficient voltage to the drive-train of the electric aircraft. The parallel connection increases the system capacity to be able to last the required flight endurance and to provide enough current to the system. As shown in equations 2.7 and 2.8, the voltage increases with respect to the number of cells in series and the capacity increase with respect to the number of cells in parallel:

$$V_{batt} = V_{cell} \cdot N_s \tag{2.7}$$

$$Q_{batt} = Q_{cell} \cdot N_p \tag{2.8}$$

In equation 2.7 and equation 2.8, V_b is the nominal voltage of battery system and the V_c is the battery cell voltage. The Q_b and Q_c are battery system capacity and the cell capacity. The N_s and N_p are the number of cells in series and number of cells in parallel. For any electric propulsion system, the voltage and capacity are dependent variables due to the dynamic properties of the battery. The V_b and Q_b are unknown parameters which need to be sized by different algorithms in the later chapters according to the proposed sizing method.

2.1.3 Battery Energy Equation

In electrical terms, the energy equals to the integral of the product of voltage and current over time. Batterys output electrical energy can be illustrated in the equation:

$$E_{batt} = \int_0^T V(t) \cdot I(t) dt \tag{2.9}$$

Equation 2.9 shows the relation between the energy of the battery in terms of battery terminal voltage $V(t)$ and discharging current $I(t)$.

2.1.4 Lithium-Ion Battery Voltage Dynamics

One of the battery pack sizing criteria is to supply sufficient power to the electric drivetrain. At any time, the power is the product of voltage and current. Therefore, the voltage dynamics of the Lithium-Ion battery is essential to accurately size the system for a propulsive battery pack application. The voltage profile throughout a battery discharge cycle is usually supplied by the battery manufacturer, such as the one shown in figure 2.2.
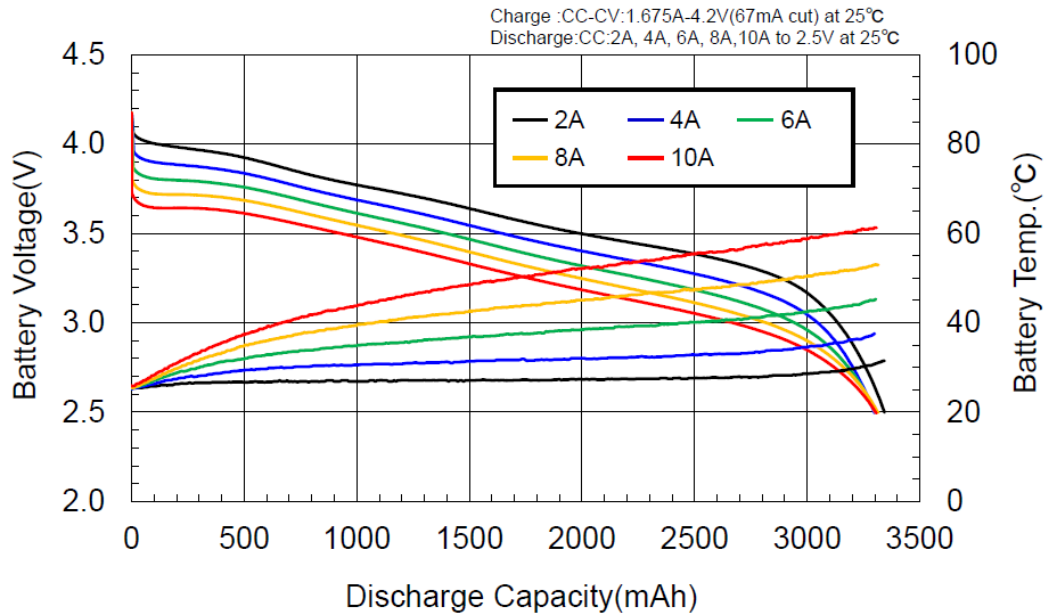
Figure 2.2 Battery Voltage Vs. Discharge Capacity at Different Discharging Rate of NCR-18650GA Battery (Panasonic, 2016).

As seen, the Lithium-Ion's voltage will vary based on discharging current and the state of charge (SOC). It can be seen that the battery's voltage decrease with respect to the

increasing discharging current and the increasing discharged capacity (Zhang & Zhang, 2015).

2.1.5   Battery Performance Linearization

Due to the complexity of the battery voltage dynamics, local linearization is usually utilized to estimate the battery's open circuit voltage (OCV) - SOC model. Within the local linearizing range, the error is less than 5% in certain scenarios (Chen & Chuang, 2017).

Researchers use the battery local linearization accompanied with extended Kalman-filter to estimate the battery SOC. In this thesis, the focus is to utilize local linearization to characterize the voltage dynamics. Therefore, the output variable will be battery terminal voltage and input variables shall be battery SOC and discharging current. As shown in 2.2, the linearization region chosen shall be the quasi-linear range of the curve to ensure the local linearization's accuracy.

2.2   Battery System Sizing Strategies

The development of advanced battery technology enables more possibility for the use of battery systems. In the aviation industry, due to weight-sensitive characteristics, an optimal battery system design for aircraft requires minimal weight. Many researchers are aiming to reduce weight for sizing battery systems.

2.2.1 Battery System Sizing by Weight Fraction

Propulsive battery systems are very popular in small unmanned aerial vehicle (UAV) developments. The vast majority of modern small UAVs are powered by batteries. Traub (Traub, 2016) used the weight fraction of the entire battery system to optimize the range or endurance of small UAV flights. In other research, Traub used a numerical method to characterize the battery voltage dynamics (Traub, 2011). By equating the battery output power to the total vehicle output power, then substituting the speed for both optimal range and endurance, he was able to obtain the optimal sizing result for both maximum endurance and range.

2.2.2 Battery System Sizing Optimization

Lithium-Ion batteries are not only common in the small UAV industries; the growth of More Electric Aircraft (MEA) is also adopting large sized Lithium-Ion battery systems in the design. The electrical structure adaptation reduces the use of bleed air from jet engines and therefore increases the efficiency.

Due to the large weight and size of such energy stored in an aircraft, the sizing requires optimal weight solution. Seanger et alias proposed a numerical optimization algorithm to size the battery system for MEAs. The algorithm requires the user to input preset conditions based on the design requirement. Then the iteration process can identify a feasible battery-supercapacitor hybrid system that has minimum weight (Saenger et al., 2017).

2.2.3   Electric Drive-Train Efficiency

Electric aircraft have an entirely novel drive-train than conventional aircraft. The electrical energy passes through components in the following sequence: the battery system, the motor controller (inverter), the electric motor, the drive shaft, and the optional gearbox. Shown in figure 2.3 is a typical electric aircraft's energy path.
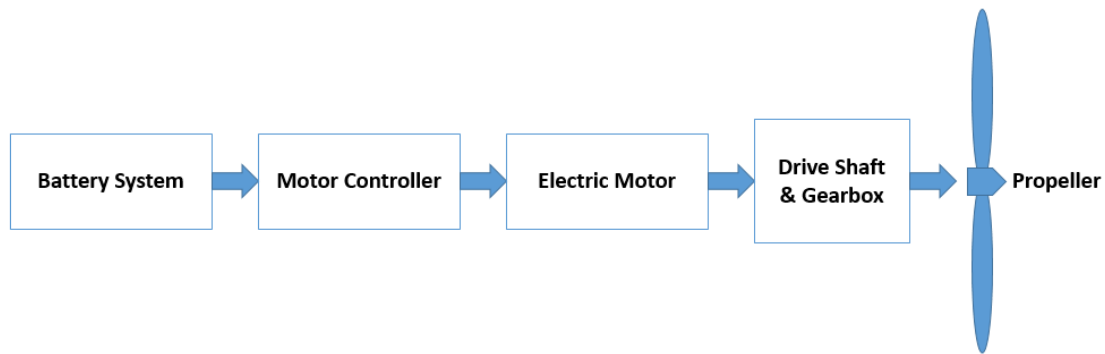
Figure 2.3 Electric Aircraft Drive-Train Illustration.

According to Lenny Gartenberg's research, the Motor Controller and electric motor have a combined efficiency map at combinations of torque and RPM. The overall efficiency is up to 93%. The electric motor manufacturer provides the efficiency map as one shown in figure 2.4. The data is essential to calculate the power required for the battery system given the power output of the electric motor.

The propeller efficiency is also needed when calculating the thrust of the electric drive-train system. The efficiency is obtained using the measurement of thrust force, rotational
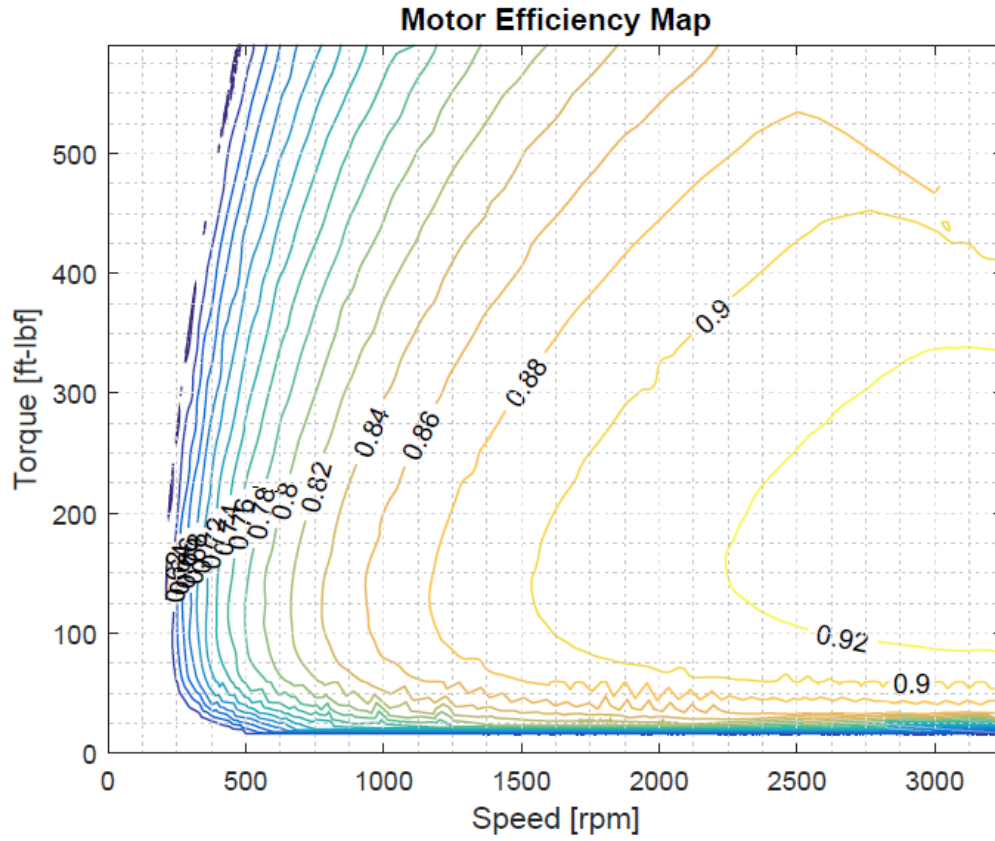
Figure 2.4 Combined Efficiency of Motor Controller and Electric Motor (YASA, 2012)

speed, and the torque exerted on the propeller. The equation for calculating the propeller efficiency is:

$$\eta_{prop} = \frac{T \cdot v}{q \cdot \omega} \tag{2.10}$$

At cruise, the lift force equals to the drag force, and the thrust can be rewritten in terms of the weight and the lift to drag ratio. Further, the engine puts out a constant RPM during cruise flight, which is indicated by the product of torque and RPM being equal to the engine cruise power setting. The propeller efficiency data is then mapped by experimental measurements and validated by calculation. The propeller used for the HK-36 project is

the MT-Propeller Model: MTV-1-A/184-51. Figure 2.5 is showing the propeller efficiency map.
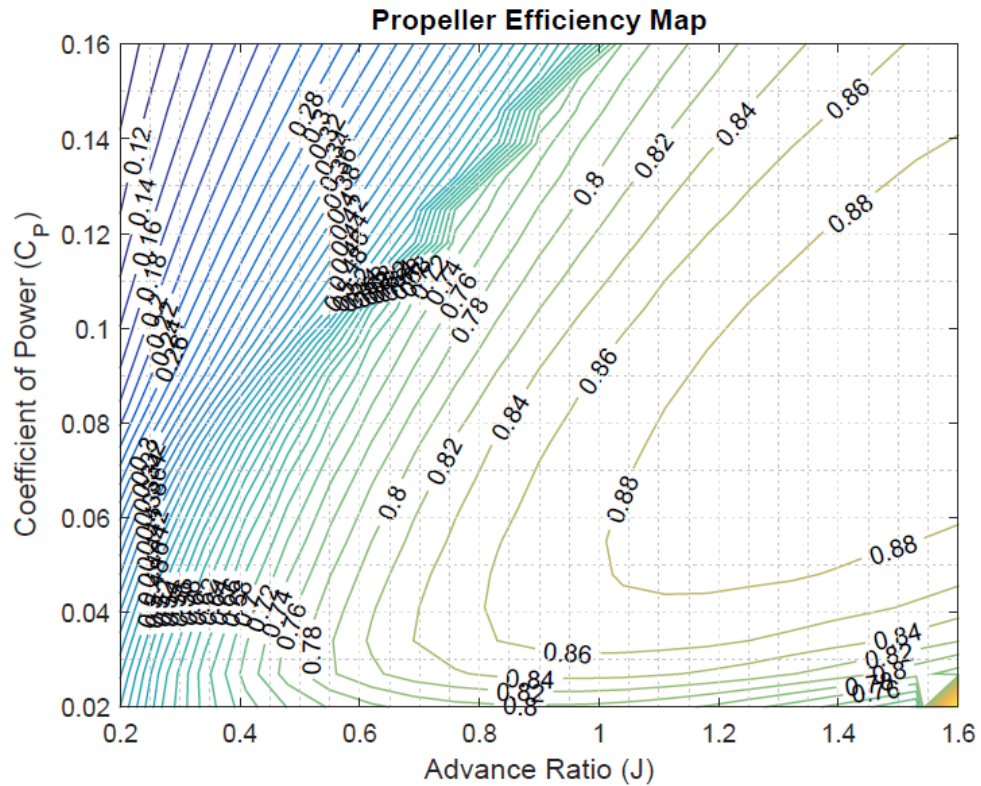
Figure 2.5 Propeller Efficiency Map (Gartenberg, 2017)

The propeller efficiency needs to be interpolated at each stage of the mission profile. The energy equation utilizes propeller efficiency value.

2.3   Battery System Weight Estimation

It is in the electric aircraft designer's best interest to have an estimated battery system weight and to bring the design into further iteration. So far, the empirical data shows 58.0% of the battery system weight is taken by the weight of the battery cell when the battery

system is using a Phase-change material cooling method. (Lilly, 2017). The estimated weight of the entire battery system will be:

$$W_B = \frac{N_p \cdot N_s \cdot W_c}{\omega_{cell}} \tag{2.11}$$

In the equation 2.11, W_B is the battery system's weight. The W_C is the weight of individual battery cell. ω_{cell} is the cell weight fraction. This weight estimation includes all the auxiliary components, such as battery pack structures, electrical connections, Battery Management System (BMS), and battery cooling system, which are all required for the battery system to function properly. The cooling method included in the weight fraction is the phase-changing composite material.

3. Methodology

3.1   Battery Cell Testing and Analysis

Battery performance can significantly change the sizing outcome of a battery system. To study the battery performance, battery cells must be put into discharging tests. These tests are designed to measure the cell voltage when varying the discharging current throughout the SOC level of the battery. By parameter identifications on the test results, the expression of battery voltage in terms battery SOC and discharging current can be found.

3.1.1   Battery Cell Testing

The equipment used in the battery cell testing is a battery tester. This equipment is able to collect battery cell's voltage, current, temperature, and discharged capacity. Figure 3.1 shows the battery testing experimental setup.

The cell test cases are constant current discharging, the test current includes 2A, 4A, 6A, 8A, and 10A. Figure 3.2 shows the single cell testing result of a Panasonic NCR-18650GA Lithium-Ion cell. One Panasonic NCR-18650GA cells in new conditions are tested. After the battery cell test is completed, test results are plotted and compiled into a two-dimensional lookup table for the battery parameter linearization.

Figure 3.1 UBA5 Battery Tester is Testing an NCR-18650 Battery Cell.
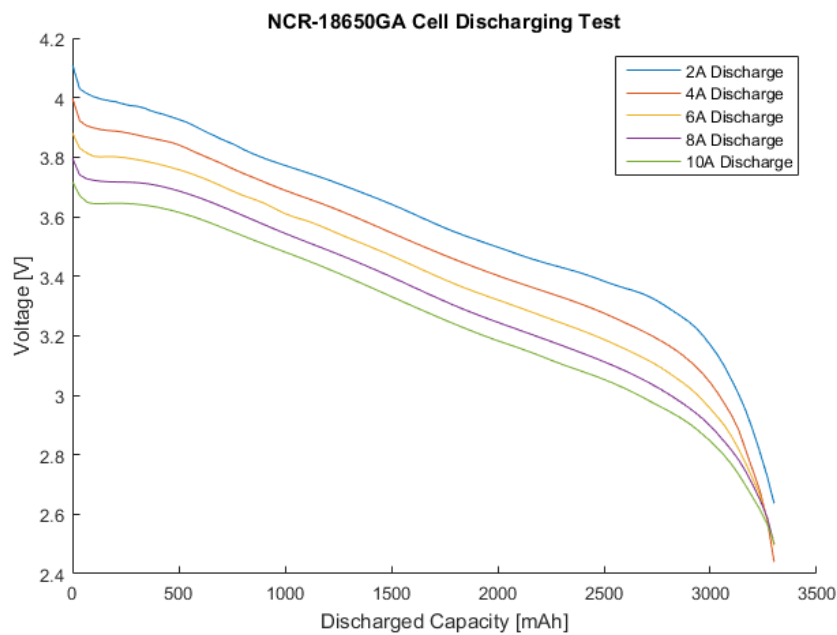
Figure 3.2 Battery Cell Test Result of Panasonic NCR-18650GA Terminal
Voltage Vs. Battery SOC Used and Discharge Current.

As seen from the battery terminal voltage curves in Figure 3.2, the battery voltage de-

creases as discharged capacity increases and discharging current increases. The expression

of battery voltage is needed for the sizing algorithms.

3.1.2 Test Parameter Linearization

By observation of the voltage behavior from Figure 3.2, it is clear that voltage behaves linearly with the majority operating range of the battery cell. The region used to generate linearized voltage equation is selected to be from 500 mAh to 2750 mAh discharged capacity. The selected region is shown in figure 3.3.
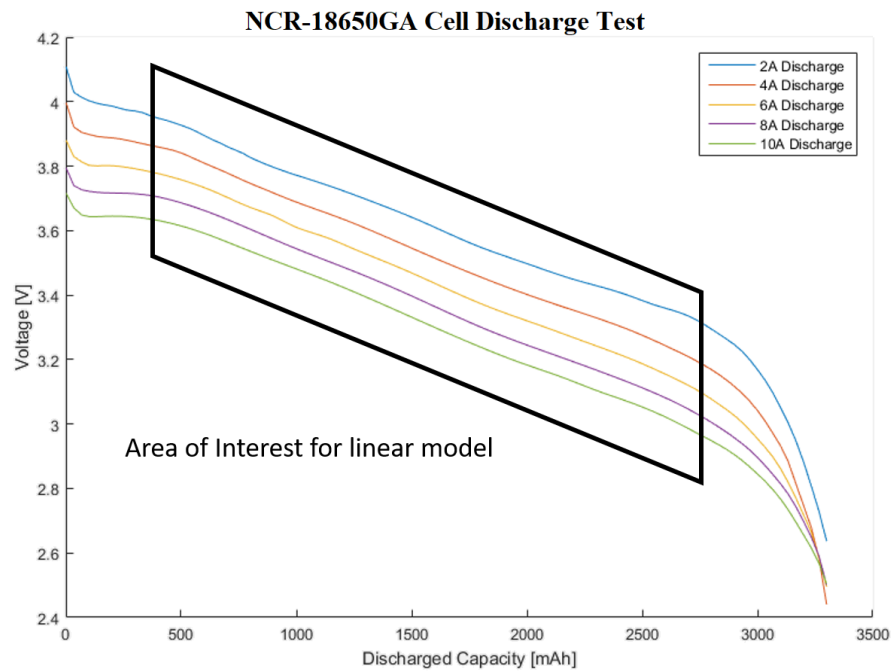
Figure 3.3 Battery Cell Test Result of Panasonic NCR-18650GA Terminal and Selected Linearized Region.

The battery test data is used to calculate the voltage equation via the least-squares regression algorithm. The Panasonic NCR-18650GA cell voltage is expressed as:

$$V = 4.14 - 0.94 \cdot SOC - 0.039 \cdot I \tag{3.1}$$

In equation 3.1, the coefficients correspond to different physical properties of the battery cell. The first coefficient, 4.14, is the battery cell voltage when the battery is at full capacity with zero discharging current, which is denoted by V_0. The second coefficient, 0.94, is the battery cell voltage decreasing rate with respect to the decrease in the remaining SOC. This is due to the decreasing of chemical-electrical potential within the battery as SOC decreases. It is denoted by V_{SOC}. The third coefficient, 0.039, is equivalent to the internal resistance R_I of the battery cell. Therefore, the battery cell voltage equation becomes:

$$V = V_0 - V_{SOC} \cdot SOC - R_I \cdot I \tag{3.2}$$

With the voltage linearized by SOC and discharging current, a comparison of test cell voltage data with the linearized cell voltage data is plotted in figure 3.4
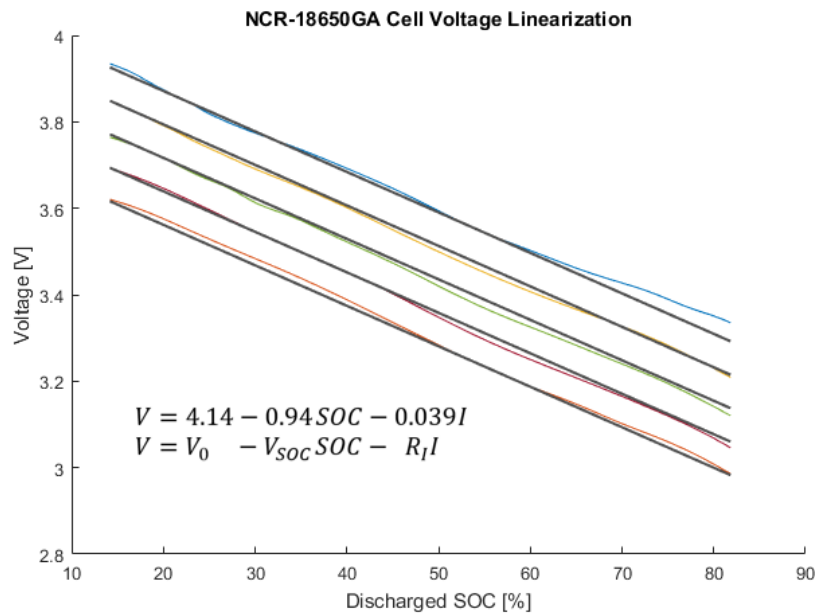
Figure 3.4 Battery Cell Test Result of Panasonic NCR-18650GA Terminal and Linearized Voltage Data.

3.2 Propulsive Battery Sizing Algorithms

The sizing process will be divided into three parts. The first part is to determine the series connection to obtain the proper system level voltage. The nominal voltage of the battery system is set to a value within the voltage operating range of the electric motor. The number of cells connected in series can then be sized. The second part is to determine the number of cells in parallel for the battery system's capacity. The capacity required for the system is further determined by either the power requirement or the endurance requirement. The third part is to combine both series and parallel sizing result to calculate the total battery number of cells. The battery system weight is then determined based on the empirical battery cell weight fraction.

3.2.1 Series Connections Sizing

The battery system sized must output appropriate voltage to the electric motor and controller such that the inverter inside the controller can operate properly. The voltage of one Lithium-Ion battery cell can be in the range from $2.5V$ to $4.2V$. The voltage of a single cell will be multiplied by Ns to become the battery system voltage, as seen in equation 2.7.

In some cases, the voltage value that the battery system outputs determines the maximum RPM the controller can drive the electric motor. This is due to the back electro-motive force (EMF) from the electric motor at higher RPM. For example, the YASA-750 Electric Motor has different RPM limits when applying different voltage, as shown in figure 3.5:
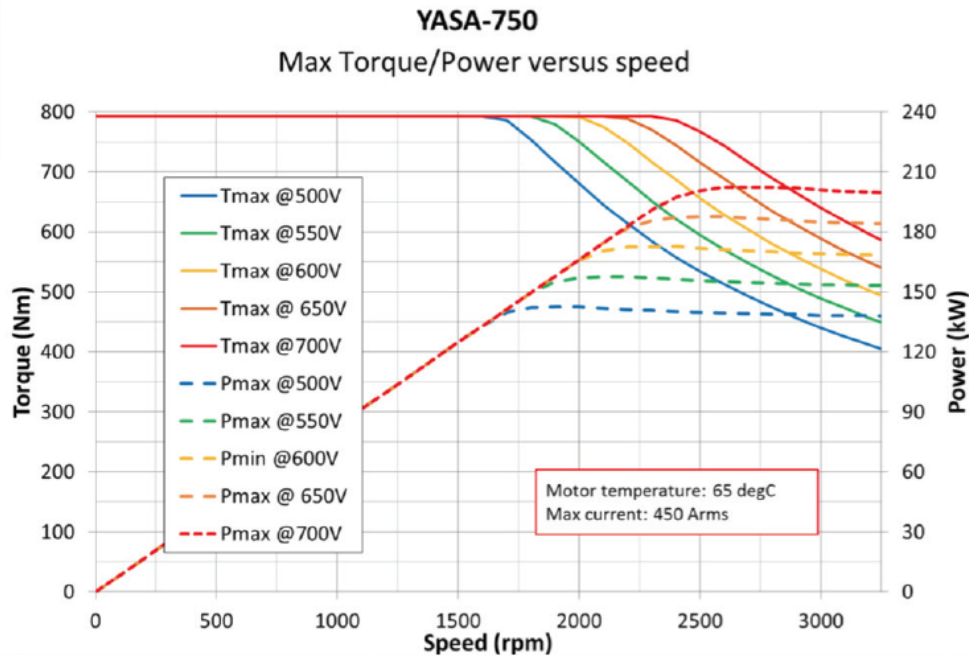
Figure 3.5 YASA-750 Electric Motor Max Torque and Power Vs. Input
Voltage and RPM (Gartenberg, 2017; YASA, 2012)

As seen in figure 3.5, the YASA electric motor has an acceptable voltage range from

500 V to 700 V to reach the peak torque. When operating at higher RPM, the available

torque decreases with respect to the supply voltage. Most electric motor controllers can

operate with a large range of input voltages.

Derived from equation 2.7, the sizing of battery cells connected in series is calculated

by the required system nominal voltage:

$$N_s = \frac{V_b}{V_c} \qquad (3.3)$$

When sizing the number of batteries connected in series, the resultant system voltage has to comply with the electric motor and controller's accepted minimum and maximum voltage:

$$N_s \cdot V_{CellMin} \geq V_{MotorMin} \tag{3.4}$$

$$N_s \cdot V_{CellMax} \leq V_{MotorMax} \tag{3.5}$$

3.2.2 Parallel Connection Sizing

The capacity of the battery system determines the number of cells needed for parallel connection. In the sizing method proposed, system capacity is designed by two main criteria: the required power and the endurance requirements. Therefore, the power method and the endurance algorithms need to be separately derived for sizing the capacity of the propulsive battery system.

Derived from equation 2.8, and after the capacity of the battery system is sized, the number of cells in parallel can be calculated as:

$$N_p = \frac{Q_{batt}}{Q_{cell}} \tag{3.6}$$

The Q_{batt} is then solved by the two proposed methods.

Required Power Sizing Method

The maximum C rate of the specific battery cell type is used in equation 2.1, the output current is in terms of the battery capacity:

$$I_{max} = C_{max} \cdot Q_{batt} \tag{3.7}$$

The current of an electric aircraft is controlled and regulated by the motor controller. Under normal operating conditions, the throttle command and the pre-programmed limitations inside the motor controller constantly regulate the current output of the battery system.

The propulsive battery system shall have built-in over-current protection. This protection is only used in emergency situations. This is due to the fact that the protection technology is normally a fuse or semiconductor switch that will be triggered when the discharge current reaches the maximum allowable current. Both types of protection can only shut off the battery pack or system as a whole instead of lowering the current output. Thus, the battery system must be sized properly to the maximum normal operating power of the electric aircraft to avoid undesired battery shutdown.

Using the maximum power of the electric motor and the efficiency of the electric motor and the motor controller, the maximum current coming out of the battery can be derived from the takeoff power efficiency equation:

$$P_{batt} = \frac{P_{mot}}{\eta_{mot}} \tag{3.8}$$

The battery system in an electric aircraft has the same about of power output via battery voltage and current:

$$P_{batt} = I_{batt} \cdot V_{batt} \tag{3.9}$$

Combining equaions 3.8 and 3.9, the battery system output current is:

$$I_{batt} = \frac{P_{mot}}{\eta_{mot} \cdot V_{batt}} \tag{3.10}$$

From here, the parallel sizing equation becomes:

$$N_p = \frac{P_{motT/O}}{\eta_{mot} \cdot V_{batt} \cdot Q_c \cdot C_{max}} \tag{3.11}$$

Finally, substituting the battery voltage dynamic model in equation 3.2, the battery sizing equation by takeoff power is

$$N_p = \frac{P_{motT/O}}{(V_0 - V_{SOC} \cdot SOC - R_I \cdot Q_{cell} \cdot C_{max})\eta_{mot} \cdot N_s \cdot Q_{cell} \cdot C_{max}} \tag{3.12}$$

In equation 3.12, the value of SOC is determined using the battery remaining percentage where the battery system is able to provide engine's full power. It is left to be arbitrarily determined by the aircraft designer.

Required Endurance Sizing Method

For endurance sizing of the propulsive battery system, the aircraft energy equation is utilized to determine the battery system's capacity. The endurance sizing method assumes that the battery power output is adequate throughout the whole flight, only additional capacity is needed for an extended endurance. To an electric propulsion system, it is also assuming that the power delivered by the battery during each phase of the mission profile is constant. This assumption is valid due to the fact that batteries are neither sensitive to airspeed nor altitude. Therefore, for simplicity, the energy used at takeoff and climb are combined as $E_{T/O}$. For cruise phase, the energy consumed is denoted as E_{Cr} The energy equation is written as the sum of the energy used for takeoff and the energy used for the cruise:

$$E_{batt} = E_{T/O} + E_{cr} \tag{3.13}$$

The energy being used for takeoff and climb depends on the aircraft's designed maximum power, and the combined time for takeoff and climb:

$$E_{T/O} = \frac{P_{motT/O} \cdot t_{T/O}}{\eta_{mot}} \tag{3.14}$$

With known total weight of the aircraft W_o and the glide ratio $\frac{L}{D}$, assuming straight and level flight for the cruise and steady power delivery, the lift equals to the weight, and the aircraft thrust will be:

$$T_{cr} = D_{cr} = W_o (\frac{L}{D})^{-1} \tag{3.15}$$

Therefore, the power required output from battery system for cruising is then:

$$P_{battCr} = \frac{v_{cr} \cdot W_o \cdot (\frac{L}{D})^{-1}}{\eta_{mot} \cdot \eta_{prop}} \tag{3.16}$$

In equation 3.16, the variable $\eta_{mot} \eta_{prop}$ takes consideration of the efficiency of the entire electric aircraft drive-train, including the motor and propeller. The resultant energy is required from the battery system.

The cruise phase energy consumption is now a function of the aircraft glide ratio, the weight of the aircraft and the required endurance time for cruising.

$$E_{Cr} = \frac{t_{cr} \cdot v_{cr} \cdot W_o \cdot (\frac{L}{D})^{-1}}{\eta_{mot} \cdot \eta_{prop}} \tag{3.17}$$

Reviewing equation 2.9, the battery energy is unresolved due to the unknown voltage and current behavior of the battery. In this case, the nominal voltage of the battery cell should be used as defined, which as the battery OCV when the battery is at half SOC. The battery energy equation becomes:

$$E_{batt} = \int_0^T V(t) \cdot I(t) dt \tag{3.18}$$

$$E_{batt} = V_{nom} \cdot \int_0^T I(t)dt \qquad (3.19)$$

Recall that the battery capacity is defined as the electric charge that the battery can contain. The battery capacity is equal to the integration of the discharge current over time. This property of battery makes the battery energy equation becomes:

$$E_{batt} = V_{nom} \cdot Q_{batt} \qquad (3.20)$$

Substituting the components in equations 3.13 with equations 3.20 3.14, and 3.17:

$$V_{nom} \cdot Q_{batt} = \frac{P_{motT/O} \cdot t_{T/O}}{\eta_{mot}} + \frac{t_{cr} \cdot v_{cr} \cdot W_o \cdot \left(\frac{L}{D}\right)^{-1}}{\eta_{mot} \cdot \eta_{prop}} \qquad (3.21)$$

Then the battery system capacity Q can be solved:

$$Q_{batt} = \frac{P_{motT/O} \cdot t_{T/O}}{V_{nom} \cdot \eta_{mot}} + \frac{t_{cr} \cdot v_{cr} \cdot W_o \cdot \left(\frac{L}{D}\right)^{-1}}{V_{nom} \cdot \eta_{mot} \cdot \eta_{prop}} \qquad (3.22)$$

Dividing the two sides of the equation by the capacity of each individual cell, the parallel number of cells sized by endurance is now:

$$N_p = \frac{P_{motT/O} \cdot t_{T/O}}{Q_{Cell} \cdot V_{nom} \cdot \eta_{mot}} + \frac{t_{cr} \cdot v_{cr} \cdot W_o \cdot \left(\frac{L}{D}\right)^{-1}}{Q_{Cell} \cdot V_{nom} \cdot \eta_{mot} \cdot \eta_{prop}} \qquad (3.23)$$

If the power output from electric motor P_{motCr} is known for cruise condition, then the equation 3.23 can be simplified as:

$$N_p = \frac{P_{motT/O} \cdot t_{T/O} + P_{motCr} \cdot t_{Cr}}{Q_{Cell} \cdot V_{nom} \cdot \eta_{mot}} \qquad (3.24)$$

3.2.3   Combined Propulsive Battery System Sizing

The total number of cells sized is the product of the number of cells in series and in parallel. The parallel sizing methods for power and endurance are both derived. The

resultant sizing for an electric aircraft sizing is then the larger number of cell in parallel. The power sizing method will ensure that the battery system is able to provide the full power. The endurance sizing method will ensure the battery system has sufficient energy to perform the entire flight profile.

$$N_t = N_s \cdot max(N_{p_E}, N_{p_P}) \tag{3.25}$$

3.3 Battery Discharging Simulation

A battery discharging simulation model is necessary for validating the sizing results. The simulation model is built based on the battery cell parameters, the proposed battery loading profile, and the sizing results to simulate the battery's performance. The simulation can output real-time battery voltage, discharge current, C rate, and state of charge.
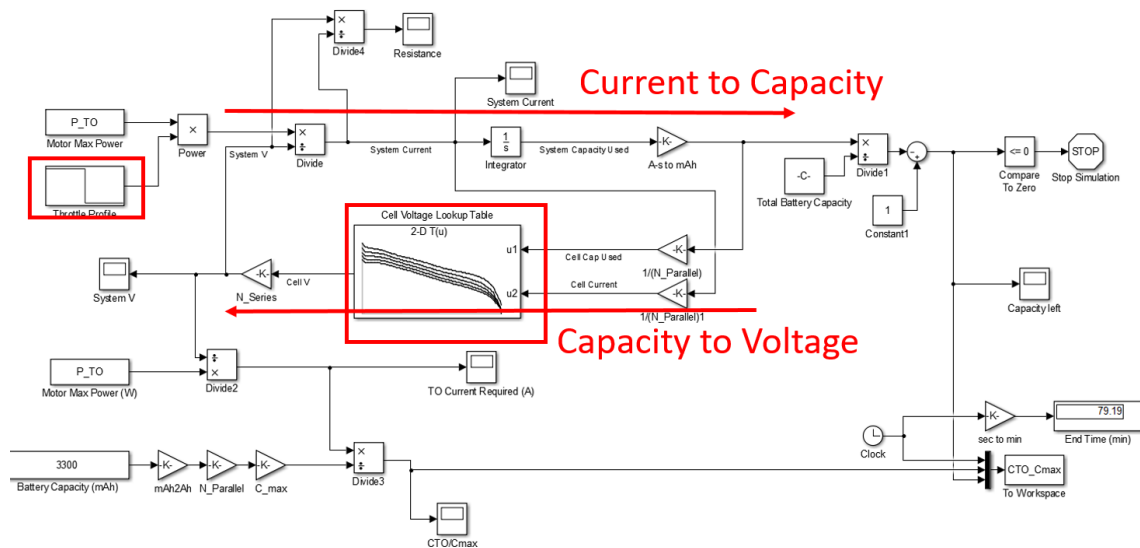
Figure 3.6 Battery Discharge Simulation Model by Simulink.

The simulation calculates the battery SOC by integrating current draw from the battery. The model then interpolates the voltage of the battery cell from the battery data lookup table. The current output of the battery is based on the voltage of the battery and the battery loading profile. The simulation can compare the dynamic C rate of the battery and the anticipated C draw at the defined loading profile. The ratio between C and C_{max} can be used to visualize the battery loading condition. The ratio $C/C_{max} \leq 1$ means that the battery discharge current is less than the battery maximum C rate. When $C/C_{max} \geq 1$, the battery output current is larger than the maximum specified current, which will result in damage or danger to the battery system.

3.4   Propulsive Battery Pack Sizing Zones

By analyzing the propulsive battery simulation results, there exist zones and boundary cases between different sizing zones. Each sizing zone corresponds to the power sizing and endurance sizing, similar to the parallel sizing methods. To make the sizing intuitive easy to understand, the zones and boundary cases need to be studied. In general, there are four zones for the battery sizing design space. The different battery performance curves are all evaluated under the same battery discharge simulation by non-dimensional parameters. The performance of the different sizing zones can be seen in figure 3.7.

3.4.1 Sizing Zones Definitions

The proposed sizing zones represent the group of sizing results that the battery system satisfies certain requirements. Each sizing zone is defined based on the phase of flight profile that the battery system able to provide the sufficient output for.

Figures have been plotted with the horizontal axis being the SOC of the battery system and vertical axis is the ratio between the battery C rate and maximum battery C rate. The line across $C/C_{max} = 1$ show the battery's maximum output current.
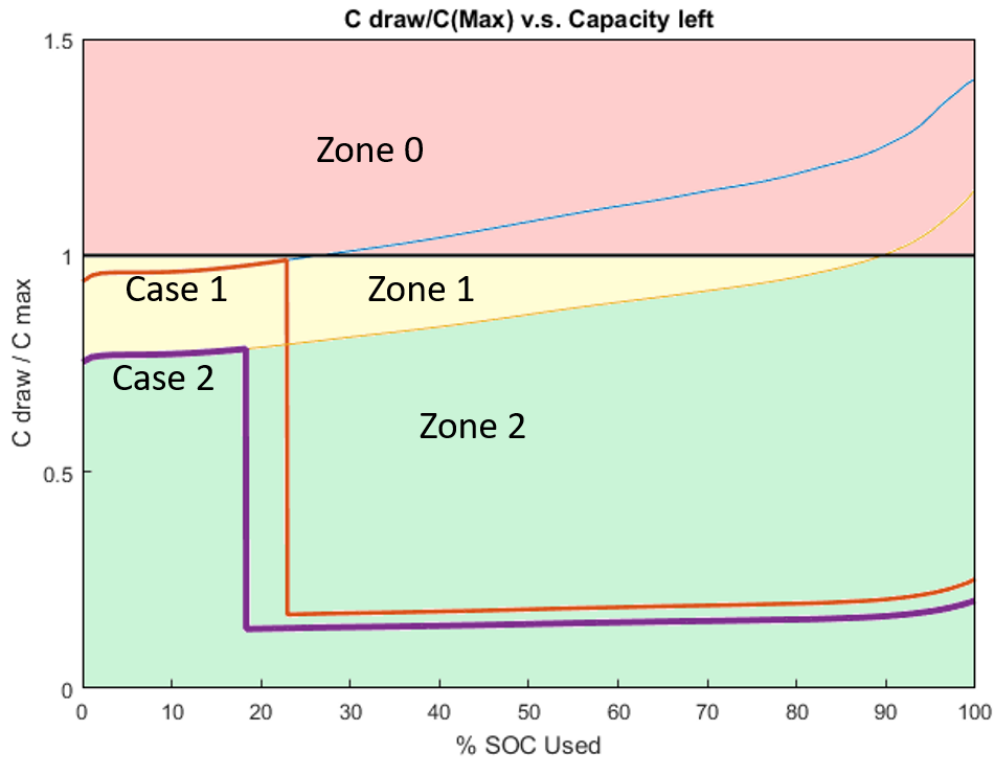
Figure 3.7 Battery Sizing Zones and Cases Definition.

First, the Zone 00 shown in figure 3.8 indicates that the sizing outcomes cannot provide the full power required even for the initial takeoff period. It is an unfeasible sizing zone.
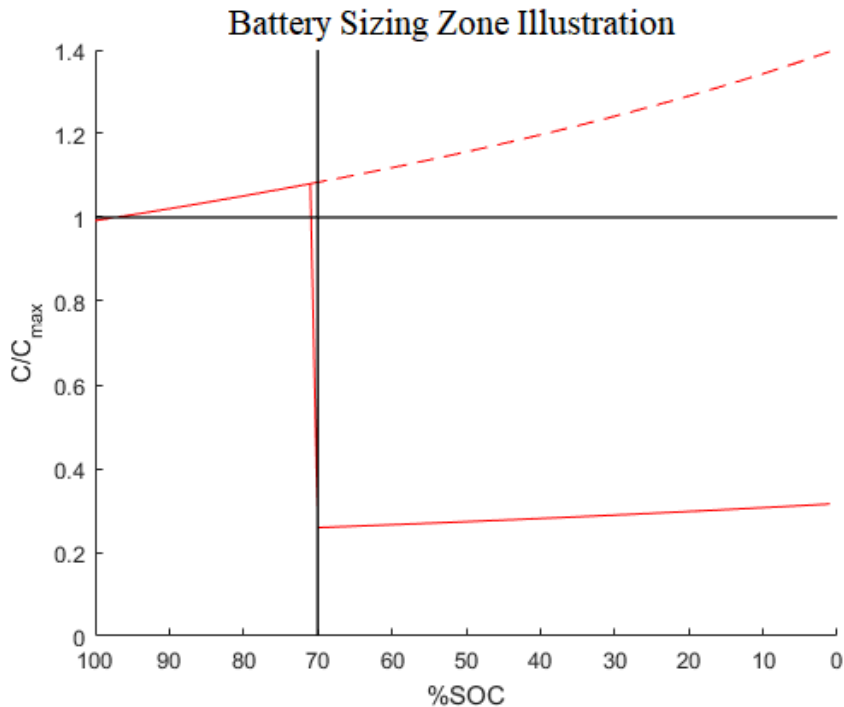
Figure 3.8 Battery Sizing Zone 00.

Second, the Zone 0 shown in figure 3.9 indicates that the sizing outcomes can provide full power during the initial takeoff period, but cannot provide the cruise power required for the cruise period due to the battery voltage dynamics. The battery systems sized within Zone 00 and Zone 0 are only feasible when the design is applied to a hybrid-electric configuration and the aircraft have additional power sources to provide the drive-train sufficient takeoff or cruise output. In reality, the Zone 0 is a rare zone to be found within the aircraft with reciprocating engines. The decrease in horsepower when switching from takeoff to

cruise will generate a larger voltage increase from the battery than the battery voltage drop throughout the SOC range.
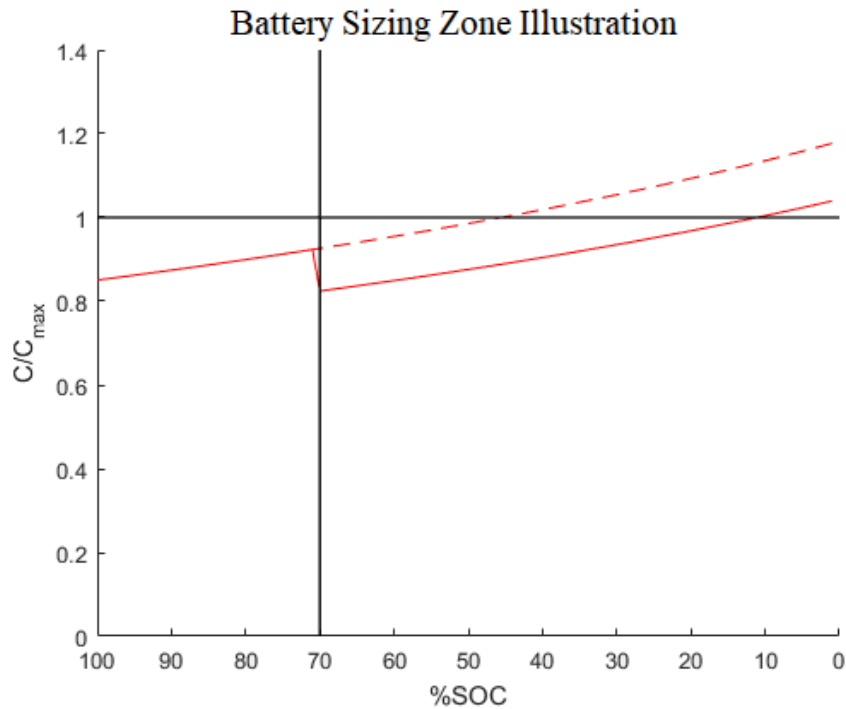
Figure 3.9 Battery Sizing Zone 0.

In Zone 1, the battery system on board an electric aircraft is generally sized for power requirements. The propulsive battery can provide the aircraft full power for the initial takeoff and climb. As shown in figure 3.10, after the initial takeoff and climb phase of the flight, the aircraft enters the cruise phase. The propulsive battery system maintains the ability to provide full power for a certain amount of the flight endurance. There is a critical SOC value that once the propulsive battery system drops below, the aircraft will lose the ability perform any full power maneuver.
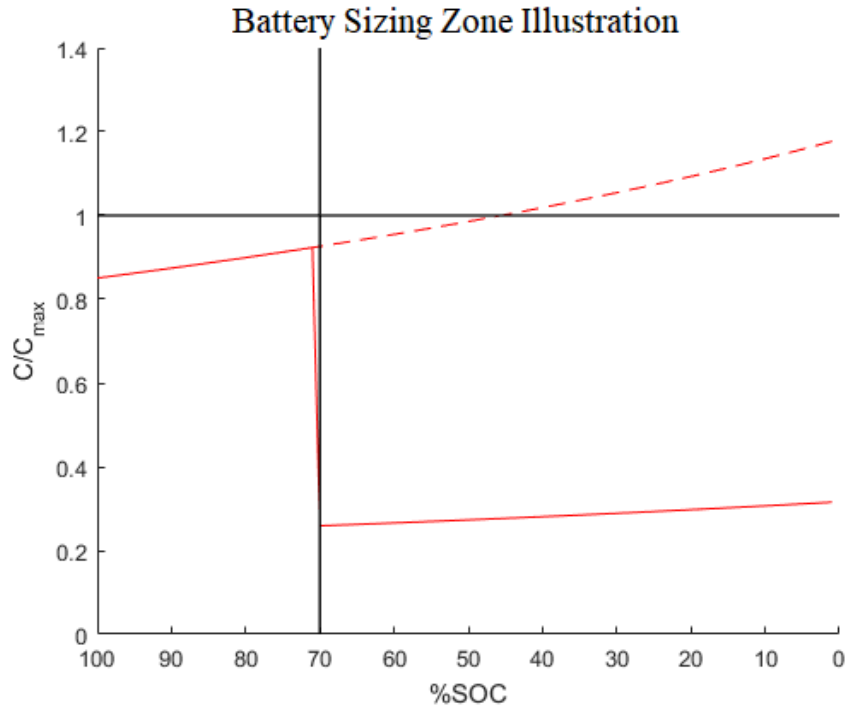
Figure 3.10 Battery Sizing Zone 1.

Lastly, Zone 2 of sizing the propulsive battery pack is shows that the current limit is never reached throughout the flight profile. Figure 3.11 shows that the battery can have full power output at any SOC. Under normal operating conditions, battery over-current protection will not be needed. When the propulsive battery is sized within Zone 2, the type of sizing must be endurance sizing.

3.4.2 Zone Boundaries and Special Cases

It is important to find out the closed form solutions for the zone boundaries and the special cases where the zones boundaries crosses to a point. The crossing points are named as Case 1, Case 2, and Case 3 in figure 3.7.
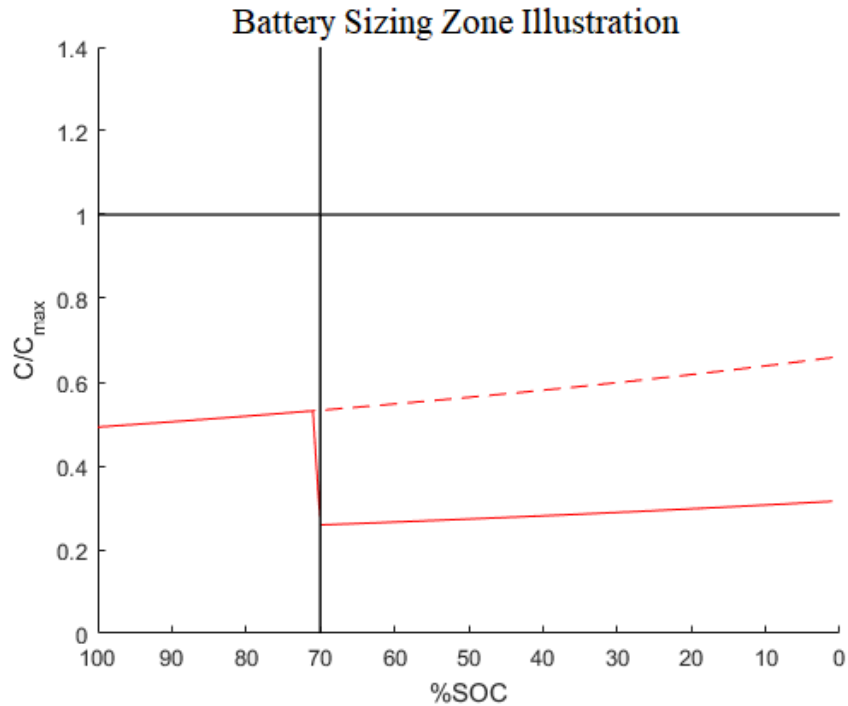
Figure 3.11 Battery Sizing Zone 2.

Case 1 is the sizing cross point at maximum battery output current between Zone 0 and Zone 1. At this sizing point, the battery system contains the exact amount of battery to allow the aircraft using full power to takeoff for the initial takeoff and climb out. Case 3 is the sizing cross point at maximum battery output current between Zone 1 and Zone 2. At Case 3 sizing point, the propulsive battery system has the exact amount of battery to make the aircraft able to perform at full power for the entire flight until the battery is depleted.

Closed-Form Sizing for Case 1: One-Time Only Full Takeoff Power

To solve Case 1 sizing point, the SOC must be found at both the end of first time takeoff and at the $C/C_{max} = 1$.

The SOC for first time takeoff is solved using energy equation:

$$E_{batt} = \frac{E_{mot}}{\eta_{mot}} \tag{3.26}$$

where

$$E_{batt} = N_s \cdot N_p \cdot Q_{cell} \cdot SOC_{T/O} \cdot V_{cell} \tag{3.27}$$

With linearized battery cell voltage, one can get:

$$E_{batt} = N_s \cdot N_p \cdot Q_{cell} \cdot SOC_{T/O} \cdot (V_0 - V_{SOC} \cdot SOC_{T/O} - R_I \cdot Q_{cell} \cdot C_{max}) \tag{3.28}$$

The electric motor consumes energy as:

$$E_{mot} = P_{T/O} \cdot t_{T/O} \tag{3.29}$$

Equating energy from equations 3.28 and 3.29,

$$N_s \cdot N_p \cdot Q_{cell} \cdot SOC_{T/O} \cdot (V_0 - V_{SOC} \cdot SOC_{T/O} - R_I \cdot Q_{cell} \cdot C_{max}) = \frac{E_{mot}}{\eta_{mot}} \tag{3.30}$$

Simplifying the equation and isolating $SOC_{T/O}$:

$$SOC_{T/O}^2 \cdot V_{SOC} + SOC_{T/O} \cdot (R_I \cdot Q_{cell} \cdot C_{max} - V_0) + \frac{P_{T/O} \cdot t_{T/O}}{\eta_{mot} \cdot N_p \cdot N_s \cdot Q_{cell}} = 0 \tag{3.31}$$

All parameters are known except for $SOC_{T/O}$. To solve $SOC_{T/O}$, the quadratic equation is used:

$$SOC_{T/O} = \frac{V_0 - R_I \cdot Q_{cell} \cdot C_{max} \pm \sqrt{(V_0 - R_I \cdot Q_{cell} \cdot C_{max})^2 - \frac{4 \cdot V_{SOC} \cdot P_{T/O} \cdot t_{T/O}}{\eta_{mot} \cdot N_p \cdot N_s \cdot Q_{cell}}}}{2 \cdot V_{SOC}} \tag{3.32}$$

Using numbers for the electrical system in the HK-36 Project, the two answers are 3.785 and 0.213. Since the value for SOC is between 0 and 1, the latter solution is chosen. The closed form equation for 1st time takeoff SOC used is:

$$SOC_{T/O} = \frac{(V_0 - R_I \cdot Q_{cell} \cdot C_{max}) - \sqrt{(V_0 - R_I \cdot Q_{cell} \cdot C_{max})^2 - \frac{4 \cdot V_{SOC} \cdot P_{T/O} \cdot t_{T/O}}{\eta_{mot} \cdot N_p \cdot N_s \cdot Q_{cell}}}}{2 \cdot V_{SOC}} \tag{3.33}$$

Next is to solve for SOC when $C/C_{max} = 1$. To do this, the C rate equation is used.

From equation 2.1:

$$C = \frac{I_{batt}}{N_p \cdot Q_{cell}} \tag{3.34}$$

Substituting equation 3.10:

$$C = \frac{P_{batt}}{V_{batt} \cdot N_p \cdot \eta_{mot} \cdot Q_{cell}} \tag{3.35}$$

Substituting equation 2.7:

$$C = \frac{P_{batt}}{V_{cell} \cdot N_s \cdot N_p \cdot \eta_{mot} \cdot Q_{cell}} \tag{3.36}$$

Replacing the V_{cell} by equation 3.4:

$$C = \frac{P_{batt}}{(V_0 - V_{SOC} \cdot SOC_{T/O} - R_I \cdot Q_{cell} \cdot C_{max}) \cdot N_s \cdot N_p \cdot \eta_{mot} \cdot Q_{cell}} \tag{3.37}$$

Formulating for C/C_{max}:

$$C/C_{max} = \frac{P_{batt}}{(V_0 - V_{SOC} \cdot SOC_{T/O} - R_I \cdot Q_{cell} \cdot C_{max}) \cdot N_s \cdot N_p \cdot \eta_{mot} \cdot Q_{cell} \cdot C_{max}} \tag{3.38}$$

Let $C/C_{max} = 1$, then:

$$1 = \frac{P_{batt}}{(V_0 - V_{SOC} \cdot SOC_{T/O} - R_I \cdot Q_{cell} \cdot C_{max}) \cdot N_s \cdot N_p \cdot \eta_{mot} \cdot Q_{cell} \cdot C_{max}} \tag{3.39}$$

To get SOC, rearrange the equation:

$$SOC = \frac{V_0 - R_I \cdot Q_{cell} \cdot C_{max} - \frac{P_{T/O}}{N_s \cdot N_p \cdot \eta_{mot} \cdot Q_{cell} \cdot C_{max}}}{V_{SOC}} \tag{3.40}$$

The next step to obtain the solution for Case 1 is to equate the SOC for first time takeoff to the SOC for $C/C_{max} = 1$. In other words, equating 3.33 and 3.40:

$$\frac{(V_0 - R_I \cdot Q_{cell} \cdot C_{max}) - \sqrt{(V_0 - R_I \cdot Q_{cell} \cdot C_{max})^2 - \frac{4 \cdot V_{SOC} \cdot P_{T/O} \cdot t_{T/O}}{\eta_{mot} \cdot N_p \cdot N_s \cdot Q_{cell}}}}{2 \cdot V_{SOC}}$$

$$= \frac{V_0 - R_I \cdot Q_{cell} \cdot C_{max} - \frac{P_{T/O}}{N_s \cdot N_p \cdot \eta_{mot} \cdot Q_{cell} \cdot C_{max}}}{V_{SOC}} \tag{3.41}$$

let

$$V'_{cell} = \frac{P_{batt}}{N_s \cdot N_p \cdot \eta_{mot} \cdot Q_{cell}} \tag{3.42}$$

and

$$V_{UL} = V_0 - R_I \cdot Q_{cell} \cdot C_{max} \tag{3.43}$$

the equation 3.41 becomes:

$$\sqrt{V_{UL}^2 - 4 \cdot V_{SOC} \cdot V'_{cell} t_{T/O}} = 2 \cdot V'_{cell} - V_{UL} \tag{3.44}$$

To solve N_p, the equation becomes:

$$N_p = \frac{P_{T/O}}{V'_{cell} \eta_{mot} \cdot N_s \cdot Q_{cell}} \tag{3.45}$$

The closed-form solution to number of cells connected in parallel at Case 1 is:

$$N_p = \frac{P_{T/O}}{(C_{max} \cdot V_0 - R_I \cdot C_{max}^2 \cdot Q_{cell} - C_{max}^2 \cdot V_{SOC} \cdot t_{T/O}) \eta_{mot} \cdot N_s \cdot Q_{cell}} \tag{3.46}$$

Closed-Form Sizing Solution for Case 3: Always Capable of Full Takeoff Power

Using similar concept, the battery sizing at case 3 can be derived using SOC_{used} equal to 90% and at $C/C_{max} = 1$. Using equation 3.38, with $C/C_{max} = 1$ and $SOC_{used} = 100\%$:

$$1 = \frac{P_{batt}}{(V_0 - V_{SOC} \cdot 90\% - R_I \cdot Q_{cell} \cdot C_{max}) N_s \cdot N_p \cdot \eta_{mot} \cdot Q_{cell} \cdot C_{max}} \tag{3.47}$$

Then number of cells in parallel for Case 3 can be calculated:

$$N_p = \frac{P_{Cr}}{(V_0 - V_{SOC} \cdot 90\% - R_I \cdot C_{max} \cdot Q_{cell}) \cdot N_s \cdot \eta_{mot} \cdot Q_{cell} \cdot C_{max}} \tag{3.48}$$

3.5 Varying System Parameter for Weight Reduction

The propulsive battery system sizing is weight sensitive. It is desired to be able to size a battery system that is able to satisfy all the design criteria and has the optimal weight savings. There are several ways to achieve this.

3.5.1 System Nominal Voltage Variation

When sizing the propulsive battery for an electric aircraft, there are a few parameters for sizing that are not influential to the general outcome of the sizing. One of the variables mentioned is the nominal voltage of the propulsive battery system. However, by only varying the system nominal voltage, the system total battery and the propulsive battery system weight will fluctuate with respect to the voltage change. The parameters in table 4.3 will be used to calculate battery sizing results using the proposed sizing algorithm to evaluate the weight change when varying the nominal system voltage.

3.5.2 Battery Cell Type Selection

Reviewing equation 3.12, the C_{max} of the Battery is defined by the battery manufacturer for safe operation of the Li-Ion Battery. The C draw of the battery is indicating the ability of the battery to the output current. When the battery sizing is power sizing, the battery C rate is then the key factor to the parallel sizing result. Next, two batteries with different C draws are used to size a general electric aircraft and the parameter is showing power sizing.

4. Result and Discussion

4.1 eSpirit of St. Louis HK-36 Electric Aircraft Propulsive Battery Sizing

To evaluate the sizing algorithm, an electric aircraft design project is needed as an evaluating example. The eSpirit of St. Louis Diamond HK-36 electric aircraft is a project at the EFRC to promote noise reduction and greenhouse gas emission for a greener future of aviation industry. The approach is to modify an existing HK-36 airframe into a fully electric aircraft. The airframe was donated to EFRC by Lockheed Martin. The electric motor chosen is a YASA-750 axial flux AC induction motor with maximum continues output of 100HP. The glide ratio of the airframe is 27:1, which means it is an aerodynamically efficient aircraft.

4.1.1 Battery System Series and Parallel Sizing

The battery system on board this HK-36 aircraft is a complete novel design by the students at Embry-Riddle. The aircraft parameters and battery information are used to evaluate the sizing algorithm proposed in this thesis.

First, The number of battery cells needed in series is calculated by using equation 3.3:

$$N_s = \frac{V_{mot}}{V_{cell}} \tag{4.1}$$

$$N_s = \frac{650V}{3.6V} \tag{4.2}$$

$$N_s = 180.5(181) \tag{4.3}$$

Second, the number of battery cells needed in parallel is calculated by power requirement. Using the power sizing equation 3.12:

$$N_p = \frac{P_{motT/O}}{(V_0 - V_{SOC} \cdot SOC - R_I \cdot Q_{cell} \cdot C_{max}) \cdot \eta_{mot} \cdot N_s \cdot Q_{cell} \cdot C_{max}} \tag{4.4}$$

$$N_p = \frac{100HP}{(4.14 - 0.94 \cdot 50\% - 0.039\Omega \cdot 3.45Ah \cdot 2.8/hr) \cdot 93\% \cdot 180 \cdot 3.5Ah \cdot 2.8/hr} \tag{4.5}$$

$$N_p = 11.46(12) \tag{4.6}$$

Third, the parallel sizing is calculated again for the endurance requirement. Equation 3.24 is used to determine numbers of cells in parallel for endurance sizing:

$$N_p = \frac{P_{motT/O} \cdot t_{T/O} + P_{motCr} \cdot t_{Cr}}{Q_{Cell} \cdot V_{nom} \cdot \eta_{mot}} \tag{4.7}$$

$$N_p = \frac{100HP \cdot 5min + 20HP \cdot 90min}{3.45Ah \cdot 3.6V \cdot 93\%} \tag{4.8}$$

$$N_p = 12.2(13) \tag{4.9}$$

The result shows that the 181 cells are needed in series connection. On the e-Spirit Electric HK-36 aircraft, the number of cells in series is 180 cells instead of 181 cells. The number is chosen due to the ability to form battery packs. Also, the 180 cells in series versus 181 cells will only create a voltage decrease of less than 1%. For ease of manufacturing and managing, the number of cells in series is decided to be 180.

Comparing the results of the endurance sizing and power sizing, the higher number shall be taken. In this case, the 13 cells from the endurance sizing. This will ensure the sizing of the propulsive battery system can satisfy both requirements. As the higher number of cells in parallel comes from the endurance sizing equation, the type of sizing is categorized as endurance sizing.

4.1.2   Combined Series and Parallel Sizing and Design Considerations

In the actual design work of e-Spirit Electric HK-36 Project, the earlier design iteration adopted the 180S x 13P for the battery cell configuration. Due to added requirements, only an even number of batteries can be connected in parallel. Thus the number of battery cells in parallel are changed to 14. The battery system that contains 180S x 13P cell will only allow all 13 cells in parallel must be grouped at the pack level. If so, a high maximum current flows through each battery pack, which makes the battery pack wiring bulky. Considering the space constraints, the engineers decided to use 7 cells in parallel inside each pack and connect two packs in parallel to make equivalent to 14 cells in parallel for the battery system.

The total number of cells used on the electric HK-36 is then

$$N_t = N_s \cdot N_p \tag{4.10}$$

$$N_t = 180 \cdot 14 \tag{4.11}$$

$$N_t = 2520 \tag{4.12}$$

The numbers of cells needed are obtained, in order to validate the sizing result, the proposed battery system is tested through the flight mission profile by the battery simulation model. Figure 4.1 is generated by the simulation. In this graph, the red curve illustrates the battery loading when tested by the given mission profile. The blue curve is simulating a constant full power being drawn from the battery system. As seen, the red curve is entirely under the $C/Cmax = 1$ line.
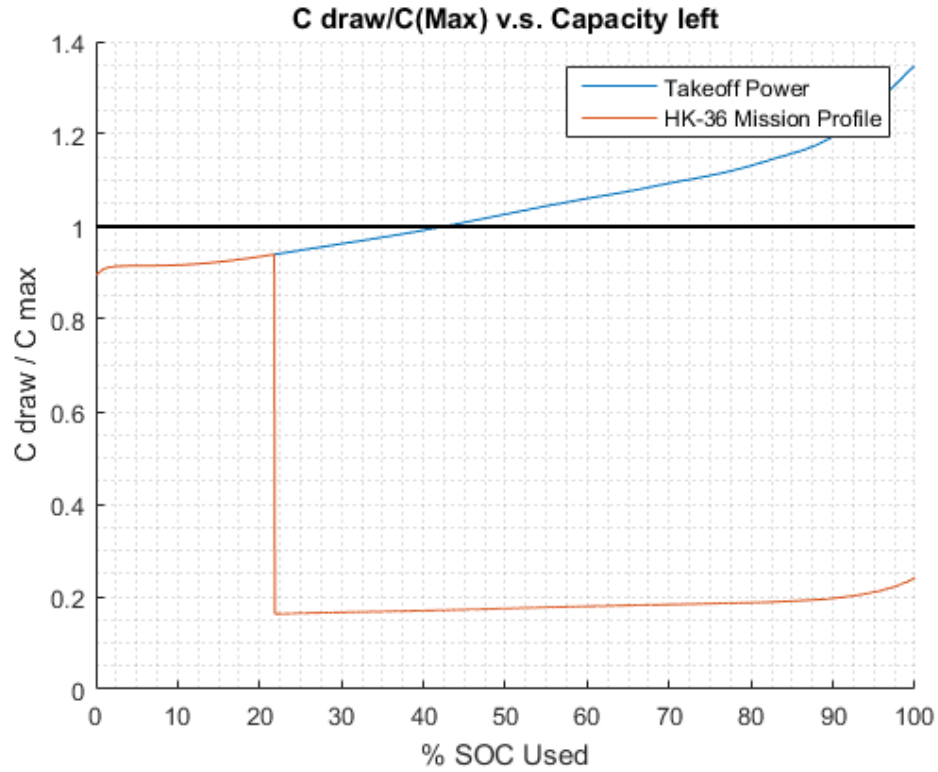
Figure 4.1 Battery Sizing Result Simulation and Validation

The battery system weight can be then estimated using the sizing result and equation 2.11. Using the sizing result, we have:

$$W_B = \frac{N_p \cdot N_s \cdot W_c}{58.0\%} \tag{4.13}$$

$$W_B = \frac{180 \cdot 14 \cdot 0.105lb}{58.0\%} \tag{4.14}$$

$$W_B = 456lb \tag{4.15}$$

As a result, the battery system on board the electric HK-36 aircraft is anticipated to be 456lb. If using the maximum takeoff weight (MTOW) of the original aircraft as the total weight with the battery system, one can find out that the battery system is occupying 26% of the weight from the entire aircraft.

4.2   Sizing Zone Boundary Solutions for HK-36 Electric Aircraft

The proposed sizing zone boundary (2 Cases) will be evaluated by using the HK-36 electric aircraft sizing parameters and the case equations. These sizing case values can intuitively show whether the sizing of the battery system is able to provide the takeoff or cruise power within the capacity of the battery system.

4.2.1   HK-36 Electric Aircraft Sizing Case 1: One-Time Only Full Takeoff Power

At Case 1, the sized propulsive battery system allows only one-time full power at the initial stage of the flight.

By applying the HK-36 electric aircraft sizing parameters to the sizing Case 1 equation 3.46:

$$N_p = \frac{P_{T/O}}{(C_{max} \cdot V_0 - R_I \cdot C_{max}^2 \cdot Q_{cell} - C_{max}^2 \cdot V_{SOC} \cdot t_{T/O})\eta_{mot} \cdot N_s \cdot Q_{cell}} \tag{4.16}$$

$$N_p =$$

$$\frac{100HP}{(2.8/hr \cdot 4.14V - 0.039\Omega(2.8/hr)^2 3.45Ah - (2.8/hr)^2 0.94 \cdot 5min) \cdot 93\% \cdot 180 \cdot 3.45Ah} \tag{4.17}$$

$$N_p = 13 \tag{4.18}$$

For the propulsive battery packs on board the HK-36 electric aircraft, the number of cells in parallel has to be equal to or larger than 13.

4.2.2 HK-36 Electric Aircraft Sizing Case 2: Always Capable of Full Takeoff Power

Case 2 is when the propulsive battery system will be able to provide full power until the battery is discharged completely. The battery sizing parameters are applied to equation 3.48 Case 2:

$$N_p = \frac{P_{Cr}}{(V_0 - V_{SOC} \cdot 90\% - R_I \cdot C_{max} \cdot Q_{cell}) \cdot N_s \cdot \eta_{mot} \cdot Q_{cell} \cdot C_{max}} \tag{4.19}$$

$$N_p = \frac{100HP}{(4.14V - 0.94V \cdot 90\% - 0.039\Omega \cdot 2.8/hr \cdot 3.45Ah) \cdot 180 \cdot 93\% \cdot 3.45Ah \cdot 2.8/hr} \tag{4.20}$$

$$N_p = 15.8(16) \tag{4.21}$$

4.3 General Aircraft Types Sizing Result

In the interest of pushing the growth of green aviation, the battery sizing algorithm is demonstrated upon various general aviation aircraft. This will help to estimate the battery system size and weight if electric-drive retrofitting is desired for the given aircraft. The aircraft types chosen do not imply any preference. In the table 4.1 below, five popular aircraft types are selected from single engine two-seats aircraft to twin-engine 6-seats aircraft.

Battery sizing algorithms have been evaluated upon the given aircraft types. The cell type chosen is the Panasonic NCR-18650GA Lithium-Ion Batteries. All of the battery pack sizings assumed five minutes full power followed by 1.5 hours endurance.

As seen in the table 4.2, the electrifications of GA aircraft are only feasible to high-efficiency airframes. Aircraft types that are equipped with high power power-train will

Table 4.1 Battery Sizing Input of Various General Aviation Aircraft (Gunston, 2015)

Airframe	Type	MTOW [lb]	$P_{T/O}$ [HP]	P_{Cr} [HP]
Diamond DA-20	1 Engine 2 Seats	1,764	125	56.3
Diamond DA-40	1 Engine 4 Seats	2,646	180	81.0
Beach A-36	1 Engine 6 Seats	3,600	285	128
Diamond DA-42	2 Engine 4 Seats	4,407	340	119
Piper PA-60	2 Engine 6 Seats	6,029	580	435
Extra EA-300	1 Engine 2 Seats	1,389	300	135

require a large number of batteries in order to meet the performance requirements. In the extreme case of Extra EA-300 aircraft, a shortened endurance must be considered.

Table 4.2 Battery Sizing Result of Various General Aviation Aircraft

Airframe	Total Cells	Battery Weight [lb]	Weight Frac.
Diamond DA-20	5800	859	48.7%
Diamond DA-40	8200	1215	45.9%
Beach A-36	13000	1926	53.5%
Diamond DA-42	12400	1836	41.7%
Piper PA-60	42000	6218	103%
Extra EA-300	13800	2043	147%
Extra EA-300 (10 min endurance)	6600	978	70.4%

As seen in the table 4.2, the electrifications of GA aircraft are only feasible to high-efficiency airframes. Aircraft types that are equipped with high power power-train will require a large number of batteries in order to meet the performance requirements. In the extreme case of Extra EA-300 aircraft, a shortened endurance must be considered.

4.4   Propulsive Battery System Weight Reduction Evaluation

By varying system parameters such as battery system nominal voltage or the change the cell type, different sizing results can be obtained. The sizing difference provides the possibility to reduce the weight of battery system which will benefit the electric aircraft design.

4.4.1   System Nominal Voltage Manipulation

Battery sizing always results in an integer for the number of cells in series and parallel. The sizing usually consists of a large number of cells in series and in parallel. When the design requirements are satisfied, both of the series and parallel sizing results are rounded up from fractions to the next integer. Within the voltage acceptable range, the battery system voltage can be manipulated to introduce a fluctuation of total battery sizing results.

Using the electric HK-36 aircraft as an example, the system nominal voltage is independent sizing variable within 650V to 700V. Within this range, various arbitrary chosen nominal voltages are used for sizing.

Table 4.3 Battery Sizing Input for Various System Nominal Voltage

Required Battery Sizing Parameters	Variable	Value	Unit
Takeoff Power	$P_{battT/O}$	107.5	HP
Takeoff Time	$t_{T/O}$	5	Min
Cruise Power	P_{battCr}	20.0	HP
Cruise Time	t_{Cr}	90	Min
Battery Nominal Voltage	V_{nom}	**600-700**	V
Capacity Required for T/O Power	$Q_{T/O}$	50	%
Cell Nominal Voltage	V_{cell}	3.6	V
Cell Capacity	Q_{cell}	3450	mAh
Cell C Rating	C_{max}	2.8	/hr

The table 4.6 shows the result from by varying the nominal system voltage for the electric HK-36 aircraft sizing. As seen, by only varying the system nominal voltage, the weight fluctuation is obvious. The discrete property of integer sizing provides the opportunity for battery weight reduction. In this example, the maximum observed weight change is 26lb between the nominal voltage of 660V and 700V. Therefore, the electric aircraft designer shall take the significance of the weight fluctuation generated by the nominal voltage selection.

Table 4.4 Battery Sizing Results Summary with Various Nominal Voltages

Sizing Parameters	600V System	650V System	680V System	700V System
Series Cells	167	181	189	195
Parallel Cells	15	13	13	13
Total Cells	2505	2353	2457	2535
Est. Battery Weight	372 lb.	349 lb.	365 lb.	376 lb.

4.4.2 Battery Cell Type Selection

Reviewing equation 3.6, one can find out that the variable C_{max} is necessary to size the propulsive battery parallel sizing. The C_{max} of the Battery is normally defined by the battery manufacturer for safe operation of the Li-Ion Battery. The C draw of the battery is indicating the ability of the battery to the output current. In the case when the battery sizing is power sizing, the battery C rate is then the key factor to the parallel sizing result. Next, two batteries with different C draws are used to size a general electric aircraft and the parameter is showing power sizing.

Table 4.5 contains a set of sizing parameters to evaluate the influence in the battery C rate when choosing different cell types. The 2.8C cell is Panasonic NCR18650GA cell, where the 8.0C cell is an LG-18650HE4 cell for demonstration purposes.

After evaluating the battery sizing cases with different C rated battery cells, the sizing results are compiled in table 4.6

Table 4.5 Battery Sizing input for Various C Rate of Battery Cell

Required Battery Sizing Parameters	Variable	Value	Unit
Takeoff Power	$P_{battT/O}$	100	HP
Takeoff Time	$t_{T/O}$	5	Min
Cruise Power	P_{battCr}	20.0	HP
Cruise Time	t_{Cr}	30	Min
Battery Nominal Voltage	V_{nom}	650	V
Capacity Required for T/O Power	$Q_{T/O}$	50	%
Cell Nominal Voltage	V_{cell}	3.6	V
Cell Capacity	Q_{cell}	3450 and 2500	mAh
Cell C Rating	C_{max}	2.8 and 8.0	/hr

Table 4.6 Battery Sizing Results Summary with Different Cell C Rates

Battery Sizing Parameter	2.8C Rate Cell	8.0 C Rate Cell
Series Cells	181	181
Parallel Cells	13	9
Total Cells	2353	1629
Type of Sizing	Power	Endurance
Estimated Battery Weight	356 lb.	232 lb.

It is obvious to notice that from Table 4.6 when the battery is sized for takeoff, the battery C Rate plays a very important role in the sizing results. The difference in between using the 2C versus 4C battery can lead to a 50% reduction in the sizing results. For applications of high power electric aircraft, endurance is a less important parameter, the high specific power types of battery shall be used accordingly.

The number used in this analysis is not representing any battery model. The values are used only to show the importance of the C rate when the battery sizing type is power sizing. Commonly, the high C rate types of battery are less suitable for endurance application. This is due to high C-rated battery often come with a lower specific energy.

4.4.3   Battery Sizing Tool Build-up

The analytical method for sizing the propulsive battery system is derived. The sizing results are tested and validated using the battery discharging simulation model. For the ease of future computation, a battery system sizing tool is developed using MATLAB GUI. The interface is shown in figure 4.2.

The tool takes inputs of battery sizing requirements, calculates the number of cells in series and parallel, and identify the type of sizing. It can also estimate the battery system weight using the empirical weight fraction data. The tool can greatly save the computation effort from the electric aircraft designer.
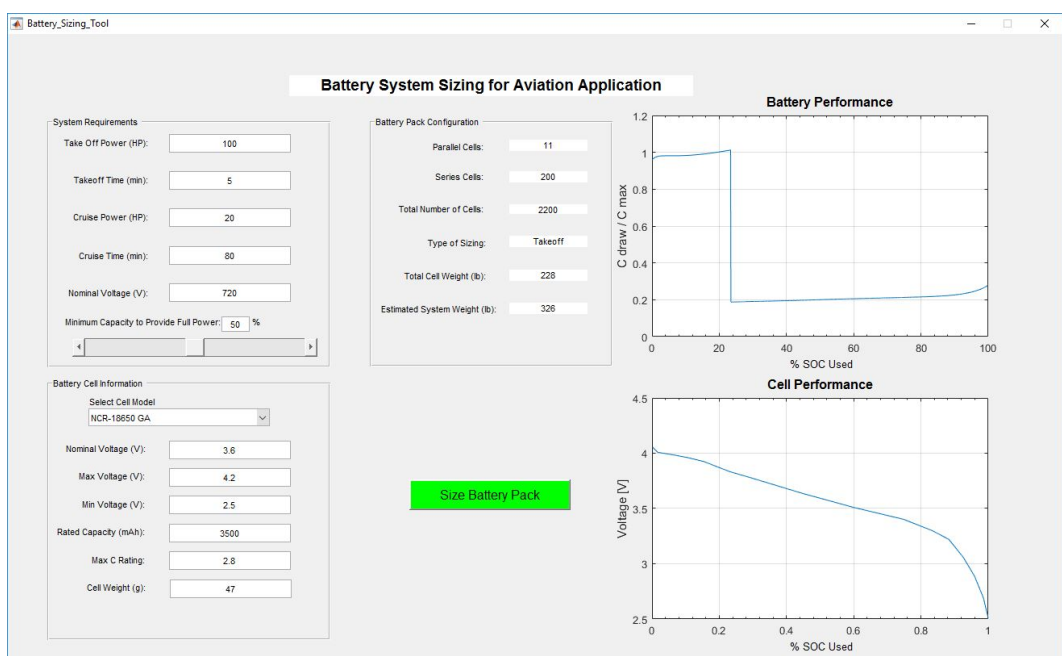
Figure 4.2 Screenshot of the Battery System Sizing Tool for Aviation Application

5. Conclusion and Suggestion

5.1 Conclusion

The propulsive battery used as an energy source for electric aircraft has significant differences from conventional propulsion energy. The analytical methods for appropriately sizing the propulsive battery system are derived. Both takeoff power and cruise endurance must be met when sizing the propulsive battery. From the sizing results, 4 zones and 2 special cases are defined. For the battery system unable to provide full takeoff power, a hybrid drive system can be considered to make up the power insufficiency. The special cases are the sizing zone boundaries. Designers can utilize the sizing special case for design trade-off study.

Based on the analysis, the cell types of battery used for different aviation applications can be varied to generate sizing fluctuations and have potential weight reduction. For battery systems that are sized for takeoff power requirement, one additional potential weight saving benefit is available if the high specific power type of battery is utilized. For other cases, when the aircraft mission requires greater cruise range or endurance, the high specific energy type of battery is preferred. The exact outcome specific battery sizing case requires further investigation. The calculation shown in this thesis can only represent the application intended for certain scenarios. The designer of electric aircraft shall consult actual sizing result to recognize the optimal solution for the particular case.

Electric aircraft using battery have tighter operating limitations than conventional aircraft. When the propulsive battery is sized to only have the ability to provide full takeoff power within certain critical SOC, operating the battery below the critical SOC value will limit the airplane from completing additional full power related maneuvers. In this case, if the electric drive-train draws a higher current from the battery system, irreversible damage to the battery system could be made. The risk of over-heating leading to thermal-runaway is also increased.

5.2 Suggestion

Due to the complexity of this research, follow-on studies are needed. Some of the points are mentioned here in order to suggest the follow-on studies.

5.2.1 Monetary and Trade-Off Study

During the selection of the cell type being used for an electric aircraft project, the designer needs to research now only the cell performance. Battery cells are relatively expensive nowadays. The cell has cycle life limitations due to the chemistry compound within the cell. Battery cell performance decreases with the cycle life increase of the cell. Therefore, battery cell's cycle life and replacement cost is also a crucial aspect of the selection basis.

5.2.2 Expanding Design Spaces

The battery cells are sensitive to its operating temperature. The cells used in very cold environment needs an additional heating device to raise the battery system's temperature in order to perform properly. The future study is suggested to include the temperature effect to the battery performance. Another important characteristic of Li-ion battery is that the cell performance will degrade throughout the cycle life. The performance analysis based on the battery's state of health is suggested in the future work for higher fidelity.

REFERENCES

Chen, B.-C., & Chuang, G.-S. (2017). State of charge estimation for lithium-ion batteries using extended kalman filter with local linearization. *SAE International*.

Exxon, M. A. (2008). *World jet fuel specifications with avgas supplement* (Tech. Rep.). Brussel, Belgium. Retrieved from `www.exxonmobileaviation.com`

Gartenberg, L. (2017). *Battery centric serial hybrid aircraft performance and design space* (Unpublished master's thesis). Embry-Riddle Aerunautical University.

Gunston, B. (2015). *Jane's all the world's aircraft 2015-2016: Development & production* (B. Gunston, Ed.). IHS Global.

Lilly, J. (2017). *Aviaiton propulsive lithium-ion battery packs state-of-charge adn state-of-health estimation and propuldive battery system weight analysis* (Unpublished master's thesis). Embry-Riddle Aerunautical University.

Panasonic. (2016). Ncr-18650ga [Computer software manual].

Saenger, P., Devillers, N., Deschinkel, K., Pera, M.-C., Couturier, R., & Gustin, F. (2017). Optimization of electrical energy storage system sizing for an accurate energy management in an aircraft. *IEEE TRANSACTIONS ON VEHICULAR TECHNOLOGY, VOL. 66, NO. 7*.

Straubel, J. (2016). Lithium-ion battery improvement rate. In *Interviewer: Fehrenbacher*.

Takaishi, T., Numata, A., Nakano, R., & Sakaguchi, K. (2008). Approach to high efficiency. *Technical Review*(Vol. 45, No. 1,), 21-24.

Tomazia, A., J. Zemva. (2013). Efficient and lightweight battery management system contributes to victory. *Electrical Power Systems Research*.

Traub, L. W. (2011). Range and endurance estimates for battery-powered aircraft. *Journal of Aircraft*.

Traub, L. W. (2016). Optimal battery weight fraction for maximum aircraft range and endurance. *Journal of Aircraft*.

YASA. (2012). Yasa 750 axial flux motor. *YASA Product Bouchure*.

Zhang, Z., & Zhang, S. S. (Eds.). (2015). *Rechargeable battries - materials, technology and new trends*. Springer.